Published OnlineFirst February 20, 2013; DOI: 10.1158/1078-0432.CCR-12-2965

Clinical Cancer Research

Quantitative Ultrasound Evaluation of Tumor Cell Death Response in Locally Advanced Breast Cancer Patients Receiving Chemotherapy

Ali Sadeghi-Naini, Naum Papanicolau, Omar Falou, et al.

Clin Cancer Res 2013;19:2163-2174. Published OnlineFirst February 20, 2013.

Published OnlineFirst February 20, 2013; DOI: 10.1158/1078-0432.CCR-12-2965

Clinical Cancer Research

Imaging, Diagnosis, Prognosis

Quantitative Ultrasound Evaluation of Tumor Cell Death Response in Locally Advanced Breast Cancer Patients Receiving Chemotherapy

Ali Sadeghi-Naini[1,2,7,8], Naum Papanicolau[1,7], Omar Falou[1,2,7,8], Judit Zubovits[4], Rebecca Dent[5,9], Sunil Verma[5,9], Maureen Trudeau[5,9], Jean Francois Boileau[6], Jacqueline Spayne[2,8], Sara Iradji[2], Ervis Sofroni[2], Justin Lee[2,8], Sharon Lemon-Wong[3], Martin Yaffe[1,7], Michael C. Kolios[7,10], and Gregory J. Czarnota[1,2,7,8]

Abstract

Purpose: Quantitative ultrasound techniques have been recently shown to be capable of detecting cell death through studies conducted on *in vitro* and *in vivo* models. This study investigates for the first time the potential of early detection of tumor cell death in response to clinical cancer therapy administration in patients using quantitative ultrasound spectroscopic methods.

Experimental Design: Patients ($n = 24$) with locally advanced breast cancer received neoadjuvant chemotherapy treatments. Ultrasound data were collected before treatment onset and at 4 times during treatment (weeks 1, 4, and 8, and preoperatively). Quantitative ultrasound parameters were evaluated for clinically responsive and nonresponding patients.

Results: Results indicated that quantitative ultrasound parameters showed significant changes for patients who responded to treatment, and no similar alteration was observed in treatment-refractory patients. Such differences between clinically and pathologically determined responding and nonresponding patients were statistically significant ($P < 0.05$) after 4 weeks of chemotherapy. Responding patients showed changes in parameters related to cell death with, on average, an increase in mid-band fit and 0-MHz intercept of 9.1 ± 1.2 dBr and 8.9 ± 1.9 dBr, respectively, whereas spectral slope was invariant. Linear discriminant analysis revealed a sensitivity of 100% and a specificity of 83.3% for distinguishing nonresponding patients by the fourth week into a course of chemotherapy lasting several months.

Conclusion: This study reports for the first time that quantitative ultrasound spectroscopic methods can be applied clinically to evaluate cancer treatment responses noninvasively. The results form a basis for monitoring chemotherapy effects and facilitating the personalization of cancer treatment. *Clin Cancer Res; 19(8); 2163–74. ©2013 AACR.*

Introduction

Breast cancer is the most frequent form of cancer diagnosed in women, second only to nonmelanoma-forming skin cancers (1). Increases in awareness coupled with the rate and efficacy of mammogram screenings has increasingly allowed for the detection of breast cancers. One-third of newly diagnosed cases have detected the presence of breast malignancies in the initial stages with tumors less than 1 cm in size (2). Although these trends do indicate a positive direction with regard to disease detection, there still remains a significant fraction of the population in which diagnosis is not made until later stages, with 5% to 20% of newly diagnosed cases being classified as locally advanced breast cancer (LABC; refs. 3, 4), and with even greater numbers outside of North America. LABC typically comprises all stage III and a subset of stage IIB (T3N0) tumors and are diagnosed as tumors that are frequently more than 5 cm, involving the chest wall, and/or classified as inflammatory breast cancer. Because of the progression of the disease and high risk for metastatic spread, patients with LABC typically have poor long-term survival rates (5-year survival rate of 55%, approximately) in comparison with the early stage patients (4).

Current methods of assessing patient responses to cancer therapy are based upon ascertaining physical measurements of the tumor during treatment. These methods include

Authors' Affiliations: [1]Imaging Research–-Physical Science, Sunnybrook Research Institute; Departments of [2]Radiation Oncology and [3]Nursing, Odette Cancer Centre; Departments of [4]Pathology and [5]Medical Oncology; [6]Division of Surgical Oncology, Department of Surgery, Sunnybrook Health Sciences Centre; and Departments of [7]Medical Biophysics and [8]Radiation Oncology, [9]Faculty of Medicine, University of Toronto; and [10]Department of Physics, Ryerson University, Toronto, Ontario, Canada

Corresponding Author: Gregory J. Czarnota, Department of Radiation Oncology and Physical Sciences, Sunnybrook Health Sciences Centre and Sunnybrook Research Institute, 2075 Bayview Avenue, T2-167, Toronto, Ontario M4N 3M5, Canada. Phone: 416-480-6100, ext. 7073; Fax: 416-480-6002; E-mail: Gregory.Czarnota@sunnybrook.ca

doi: 10.1158/1078-0432.CCR-12-2965

Published OnlineFirst February 20, 2013; DOI: 10.1158/1078-0432.CCR-12-2965

Translational Relevance

Current methods of assessing patient responses to cancer treatment are clinically based on physical measurements of the tumor. Tumor size reduction frequently requires several months of treatment administration, and in some cases, tissue diminishment is not present despite treatment response. In contrast, functional imaging methods that probe tumor physiology may be used to detect tumor responses from days to weeks after starting therapy. This study indicates, for the first time, that conventional frequency quantitative spectroscopic ultrasound can be applied to noninvasively monitor the effects of chemotherapy cancer treatment in patients with locally advanced breast cancer. We show that quantitative ultrasound techniques can be used to detect and evaluate responses of cancer patients within weeks after starting therapy. This ultrasound-based functional imaging can therefore facilitate the practice of personalized medicine for patients with cancer.

clinical examination, X-ray mammography, conventional ultrasound imaging, and MRI. Physical examination by palpation is commonly used by clinicians; however, this method of tumor assessment is subjective (5). During the course of the last several decades, X-ray mammography has made considerable improvements in the detection of breast cancers but has not shown significant promise in tracking tumor response during treatment. MRI is commonly used for assessing the end result of treatment in patients with LABC as it provides high-resolution images allowing clinicians to fairly accurately measure tumor volume. However, it remains a costly imaging modality to use. Another limitation stems from the fact that these methods attempt to ascertain patient response to treatment by determining the physical size of the tumor. Tumor size reduction, however, frequently requires several weeks to months of treatment administration and in some cases, mass diminishment is not present despite a cytotoxic treatment response (6).

Changes in tumor size with treatment are the late cumulative result of early microstructural changes in tumor cell morphology often due to cell death, starting to take place within hours to days after treatment administration. This then provides the possibility of assessing the early effects of a treatment on a tumor to monitor therapy efficacy, in advance of changes to the overall tumor volume. Thus, the advent of a noninvasive functional method to monitor patient responses to therapy would be advantageous to guide the customization of chemotherapy or other cancer therapies on an individual patient basis. Alternatively, such imaging methods could also facilitate a switch to an early salvage therapy for patients whose responses to the current therapy are determined to be limited.

Research into the potential of ultrasound to monitor noninvasively the effects of cancer therapy administration was initially conducted using high-frequency (20–50 MHz) ultrasound and showed its capacity to detect changes in tissue microstructure associated with a variety of cancer therapies in *in vitro*, *in situ*, and *in vivo* models (7–14). Initial *in vitro* observations indicated increases in tissue echogenicity in acute myeloid leukemia cells exposed to the chemotherapeutic agent cisplatin (7, 8). Further research used quantitative ultrasound techniques such as spectroscopic analysis of radiofrequency data and statistical analysis of the signal envelope to quantify the effects of treatment in a variety of concentration and exposure-dependent experiments (9, 10). To date, high-frequency ultrasound has been used to detect apoptotic cell death resulting from photodynamic, X-ray radiation, and ultrasonically activated antivascular microbubble therapies in a variety of *in vivo* mouse models (12–14). These studies showed up to 16-fold maximal increases in observed backscatter signal intensity accompanied by increases in spectral parameters such as spectral slope, 0-MHz intercept, and mid-band fit (MBF) quantitative parameters which can be related to effective scatterer size, acoustic concentration, and both, respectively (15, 16). Similar techniques have been applied previously in a variety of other ultrasound tissue characterization applications such as the differentiation of mammary carcinomas and sarcomas from benign fibroadenomas and the diagnoses of cardiac and liver abnormalities and prostate cancer (17–20).

High-frequency 20 to 50 MHz ultrasound benefits from an increased imaging resolution (30–80 μm) when compared with clinically used conventional frequencies of 1 to 20 MHz (80 μm–1.5 mm). However, it suffers from a limited tissue penetration depth, restricting its use to superficial tissue sites near the skin surface. On the other hand, while the application of conventional frequency ultrasound carries a decreased imaging resolution, it benefits from a substantive tissue penetration capacity. Such an advantage potentially allows to noninvasively monitor the effects of therapy on deeper malignant tissues such as breast, kidney, and liver tumors. This has motivated a number of recent studies into the capacity of conventional frequency ultrasound in the detection of cancer treatment effects, effectively laying the groundwork for this clinical evaluation (21–23).

In this study, the potential of conventional frequency quantitative ultrasound has been investigated for the first time to noninvasively monitor the effects of clinical cancer treatment in patients. Patients with LABC receiving neoadjuvant chemotherapy were monitored during their treatment. Conventional frequency (~7 MHz) spectroscopic ultrasound data were collected before treatment as well as at weeks one, 4, and 8 during the course of treatment, and within one week before the modified mastectomy surgery. On the basis of their ultimate clinical and pathologic response to the chemotherapy, patients were classified into 2 groups of treatment response: responders and nonresponders. Patient responses were assessed on the basis of tumor diminishment and levels of cellularity. Analysis of ultrasound data used linear regression analysis of the normalized power spectrum using a sliding window approach in

Published OnlineFirst February 20, 2013; DOI: 10.1158/1078-0432.CCR-12-2965

addition to statistical quantification of spectral parametric images. Results indicated statistically significant differences in the MBF change between patients responding to treatment and nonresponders after 4 weeks of treatment. Changes in the 0-MHz intercept exhibited similar trends between 2 groups of patients, where statistically significant differences were revealed after 4 weeks of treatment. The spectral slope parameter was found to be invariant in both groups. Statistical analysis of spectral parametric images also indicated changes which resulted in a statistically significant difference between 2 groups after 8 weeks of treatment.

This study thus indicates for the first time that conventional frequency ultrasound can be potentially used as a noninvasive technique to monitor patient responses to clinical cancer therapies within weeks of their treatment initiation. This work forms a basis for clinical application of these methods to detect and evaluate cancer patient responses to the treatments, which can consequently facilitate treatment customization or even the early switch to salvage therapy.

Materials and Methods

Study protocol and data collection

This study was conducted with research ethics approval and was open to all women with LABC ages 18 to 85 years meeting the study criteria. Ultrasound data were acquired 5 times during the course of treatment of patients. The first scan was acquired immediately before the start of chemotherapy, which was used as a baseline of comparison for subsequent scans. The following 3 scans were acquired during the first, fourth, and eighth week of treatment, with a fifth scan acquired within one week before the modified radical mastectomy surgery typically occurring 4 to 6 weeks after the course of treatment was completed.

All the ultrasound data in this study were collected by the same sonographer following standardized protocols for data acquisition. Ultrasound data was acquired with patients lying supine with their arms above their heads. Conventional B-Mode and radiofrequency ultrasound data were acquired using a Sonix RP, (Ultrasonix Vancouver) system using a L14-5/60 transducer with a transmit frequency of 10 MHz, resulting in a frequency bandwidth with a center frequency of approximately 7 MHz. The transducer focus was set at varying depths depending on the individual patient circumstances and digital radiofrequency data acquired with a sampling frequency of 40 MHz. Scan focal depths remained consistent for individual patients throughout the study. Breast regions selected for ultrasound scanning were directed by an oncologist who determined acquisition scan planes via physical examination of the patient. Data were acquired in a single continuous sweep over the tumor volume to provide context regarding changes in localization and dimensionality of the tumor across visits. Scans of individual tumor regions were also acquired at approximately 1 cm increments across the tumor volume.

Before therapy, all patients underwent a core needle biopsy to confirm a cancer diagnosis, where information regarding the tumor grade, and histologic subtype were recorded. Pretreatment imaging of patients included MRI of the breast to determine initial tumor size and to conduct a metastatic workup as necessary as part of the institutional standard of clinical care for such patients. Patients were followed clinically by oncologists who remained blinded to the study results. Physical examination was conducted at each time and tumor size was assessed by clinicians. Posttreatment MRI scans of the breast were also acquired immediately before patient surgery to measure residual tumor size. Following surgery, patient mastectomy specimens were mounted on whole-mount (24) $5'' \times 7''$ pathology slides digitized using a confocal scanner (TISSUEscope, Huron Technologies) at 2 micron resolution. All cases were examined by the same pathologist (J. Zubovits), who provided information regarding residual tumor size, grade, extent of cellularity, histologic subtype, and tumor response. Patient responses were categorized on the basis of changes in overall tumor volume determined clinically during the treatment, in addition to the residual tumor cellularity. Patients were considered responders if there was a decrease in tumor size of 30% or more and included patients which were deemed to have a complete pathologic response to treatment (no residual invasive carcinoma; ref. 25). Conversely, patients were deemed to be nonresponders if there was less than 30% decrease in tumor size and included patients with progressive disease in which the tumor volume increased despite treatment (25). In cases where the tumor cellularity was very low (overall volume of viable tumor cells), the patient was considered as a responder even if the diminishment in the physical tumor size was less than 30%. In contrast, in cases where tumor cellularity was very high, the patient was considered a nonresponder even if shrinkage in the physical tumor size was approximately 30%.

Data analysis

Ultrasound radiofrequency data analysis was conducted using linear regression analysis of the normalized power spectrum (7–15, 17–20). Ultrasound data was analyzed across all acquired planes through the scan volume which included identifiable tumor regions. Analysis parameters were reported from data within a region of interest (ROI) located at the tumor central area which was consistently positioned at the transducer focal depth, typically accounting for approximately two-third of the tumor area in cross-sectional plane.

The power spectrum was calculated using a Fourier transform of the raw radiofrequency data for each scan line through the whole field of view of the ultrasound data (described further below). To remove the effects of system transfer functions, transducer beam-forming, and diffraction artefacts, in addition to acting as a mechanism of depth-related attenuation correction, data were normalized using a sliding window analysis with the power spectrum obtained from an agar-embedded glass bead phantom model, modified from ref. (26), with properties similar to

Published OnlineFirst February 20, 2013; DOI: 10.1158/1078-0432.CCR-12-2965

those of breast tissue. Phantom data were acquired for each setting used during patient data acquisition, including variations in image gain and focal depth. Linear regression analysis was conducted within the −6 dB window centered at the transducer center frequency, which was determined from a calibration pulse, to generate a best-fit line. Parameters subsequently reported included the MBF, the spectral slope, and the corresponding 0-MHz intercept (16, 27–29). Parameters were determined for each of the scan planes collected per patient visit and subsequently averaged across the tumor volume.

Specifically, spectral parameters for each scan plane were determined through averaging on the parametric images generated using a sliding window analysis on a pixel by pixel basis. Each sliding window was normalized separately to a reference curve obtained from the same region of the phantom with equivalent location and size. This was carried out to more accurately account for the effects of attenuation and beam diffraction across the ROI especially in larger tumors. Statistical analysis was carried out on parametric images via probability density function estimation of histogram of the MBF intensity by fitting a generalized gamma distribution (10).

Comparison of each patient's data during treatment was conducted using her corresponding data acquired before the treatment administration onset, as the baseline. The values of each quantitative parameter for clinically and pathologically determined responders and nonresponders were compared independently for each time. Statistical analysis using a *t* test (unpaired, 2-sided, 95% confidence interval) was carried out to assess whether patients showing statistically significant changes in the quantitative ultrasound parameters correlated to the ultimate treatment response. Discriminant analysis (PASW Statistics 18, SPSS, Inc.) was used to determine which quantitative parameter better discriminate between responders and nonresponders. Sensitivity and specificity were calculated to measure the performance of the ultrasound treatment response classification method in comparison with clinically and pathologically determined responses.

Results

Patient characteristics and clinical/pathologic treatment response

Characteristics of the participating patients, as well as their tumor properties, and the treatments administrated are summarized in Table 1. The patients had an average age of 47 years (SD = 9.5; range, 33–72). The average size of the largest tumor dimension was 8.1 cm (SD = 2.9; range, 3–13). Among 24 patients, 11 had tumors with positive estrogen and/or progesterone receptors (ER/PR+), whereas 9 had a Her-2-Neu–positive (HER2+) status. The majority of patients received combined anthracycline and taxane-based chemotherapy.

Clinical/pathologic responses of the patients are given in Table 2. Patients 1, 4, 5, 7, 8, 10, 13, 14, 15, 16, 18, 19, 20, 21, 23, and 24 had either a complete pathologic response or had substantial reductions in their tumor size along with decreases in tumor cellularity and were categorized as responders. In the case of patients 2 and 17, the reduction in physical tumor or mass size was less than 30%; however, residual tumor cellularity was very low and these patients were clinically/pathologically classified as responders. Patients 6, 9, 11, 12, and 22 were nonresponders. They showed progressive disease or their tumor size only slightly changed during treatment. In the case of patient 3, while the reduction in tumor size was slightly more than 30%, the tumor cellularity in the residual mass remained very high. As such, this patient was also classified as a nonresponder clinically and pathologically.

Quantitative ultrasound evaluation of treatment response

Representative ultrasound B-mode images, and the spectral parametric images, acquired from a responding patient with LABC tumor before the start of chemotherapy onset, and after 4 weeks of treatment, are presented in Fig. 1A. An overall increase in the ultrasound spectral backscatter power was detectable within the tumor region, as also presented in the MBF and 0-MHz parametric images. Normalized power spectra and generalized gamma fits on the histograms of the MBF intensity for the representative tumor region are also presented in Fig. 1B. Figure 1C shows representative 0-MHz intercept parametric images corresponding to nonresponder and responding patients, acquired from the same nominal breast tumor regions during treatment. Although considerable changes were visualized over the course of treatment in the parametric images that correspond to the responding patients, no such striking change was observed in the case of the nonresponding patient. Representative light microscopy images of whole-mount histopathology obtained following modified radical mastectomy surgery are given in Fig. 2 for a responding and a nonresponding patient. Contrary to the case of the responding patient, the whole-mount histopathology sample corresponding to the nonresponding patient indicates a large compact residual mass in the mastectomy specimen, in both hematoxylin and eosin (H&E)-stained slide and the slide stained to highlight ER+ areas. There were differences also observed in the trend of their corresponding MBF parameters measured over the course of treatment for these patients. Although the responding patient exhibited an average increase of up to approximately 19 dBr (logarithmic unit for normalized power relative to a reference phantom) in MBF at weeks 4 to 8 of chemotherapy, the nonresponding patient did not show such a considerable change (only up to ∼5 dBr) in this quantitative parameter during the course of treatment.

Average data obtained from treatment responding and nonresponding patients over the course of treatment is presented in Fig. 3. The results indicate a substantial increase in the ultrasound spectral backscatter power acquired from the patients that responded to the treatment. Mean increases in MBF in responding patients were measured as 3.5 ± 1.1 dBr, 9.1 ± 1.2 dBr, 8.6 ± 1.4 dBr, 1.2 ± 2.3 dBr in the first, fourth, eighth week of treatment, and preoperatively, respectively. Results from patients who did not

Published OnlineFirst February 20, 2013; DOI: 10.1158/1078-0432.CCR-12-2965

Table 1. Patient characteristics

Patient	Age	Menopausal status	Pretreatment tumor dimensions (AP × ML ×SI) in cm	Histology	Grade	ER/PR	Her-2-neu	Neoadjuvant treatment
1	55	N/A	5.4 × 5 × 2.3	Ductal	N/A	−	+	FEC+ paclitaxel, trastuzumab
2	53	N/A	7.4 × 7	Ductal	2	+	−	Epirubicin, docetaxel
3	41	Premenopausal	4	Ductal	3	+	+	Docetaxel, carboplatin, trastuzumab
4	65	Postmenopausal	10 × 10	Ductal	2	−	−	AC + docetaxel
5	50	Premenopausal	4 × 5	Ductal	N/A	−	+	AC + docetaxel, trastuzumab
6	46	N/A	7 × 8	Ductal	3	−	−	AC+ paclitaxel
7	33	Premenopausal	5.4 × 5 × 8	Ductal	N/A	+	+	AC + docetaxel, paclitaxel, trastuzumab
8	48	Postmenopausal	4.9 × 4.9 × 4.1 & 3.2 × 1.3 × 2.9	Ductal	2	+	−	AC + docetaxel
9	36	Premenopausal	4.4 × 3.9 × 5.8	Ductal	2	+	−	AC + paclitaxel
10	40	Premenopausal	4.4 × 3.4	Ductal	3	−	−	AC + paclitaxel
11	38	Premenopausal	7.5 × 4.9 × 9.2	Ductal	2	+	−	AC + paclitaxel
12	53	N/A	8.4 × 9.4 × 12.7	Metaplastic	3	−	−	AC + cisplatinum, gemcitabine platinum
13	50	Premenopausal	13 × 11	Ductal	3	−	−	AC + paclitaxel
14	49	Premenopausal	7.1 × 5.5 × 8.9	Ductal	3	−	+	Docetaxel, trastuzumab
15	40	Premenopausal	3 × 2.4 × 3	Ductal	3	+	+	AC + paclitaxel, trastuzumab
16	49	Premenopausal	2.4 × 2.8 × 1.4 & 1.4 × 2.8 × 1.3	Ductal	3	−	+	AC + paclitaxel, trastuzumab
17	47	Premenopausal	5.2 × 4 × 4	Ductal	2	+	−	FEC+ docetaxel
18	38	Premenopausal	9 × 6.6 × 6	Ductal	2	+	−	AC + paclitaxel
19	36	Premenopausal	13 × 12	Ductal	1	+	−	Dose-dense AC + paclitaxel
20	36	Premenopausal	12.5	Ductal	N/A	−	−	Dose-dense AC + paclitaxel
21	72	Postmenopausal	10 × 8	Ductal	3	−	+	Dose-dense AC + paclitaxel
22	47	Premenopausal	8 × 10	Ductal	2	+	−	Dose-dense AC + paclitaxel
23	57	Postmenopausal	7.9 × 4.1 × 5.5	Ductal	N/A	−	−	Dose-dense AC + paclitaxel
24	47	Premenopausal	6.3 × 4.1 × 7.4	Ductal	N/A	−	+	Dose-dense AC + paclitaxel, trastuzumab

Abbreviations: AC, adriamycin and cytoxan; FEC, fluorouracil (5FU), epirubicin, and cyclophosphamide.

respond to chemotherapy were measured as 0.3 ± 1.9 dBr, 1.9 ± 1.1 dBr, 3.3 ± 1.5 dBr, −1.2 ± 4.3 dBr in the first, fourth, eighth week of treatment, and preoperatively, respectively. The 2 patient populations exhibit a statistically significant difference (unpaired *t* test, 2-sided, $\alpha = 0.05$) in changes of MBF at week 4 ($P = 0.005$) and with less significance at week 8 ($P = 0.046$) of chemotherapy. Results obtained for the 0-MHz intercept parameter followed similar trends. Mean increases of 4.0 ± 1.4 dBr, 8.9 ± 1.9 dBr, 10.8± 2.4 dBr, 2.4± 2.1 dBr were measured in positively responding patients, in the first, fourth, eighth week of treatment, and preoperatively, respectively. Results corresponding to the nonresponding patients were measured as −1.3 ± 1.4 dBr, 1.6 ± 0.9 dBr, 1.4 ± 2.7 dBr, 0.6 ± 3.2 dBr in the first, fourth, eighth week of treatment, and preoperatively, respectively. Statistical analysis of the 0-MHz intercept data indicated a statistically significant difference in the changes observed in the 2 patient populations at the fourth ($P = 0.041$) and eighth ($P = 0.046$) week of treatment. The spectral slope parameter remained almost invariant within the 2 patient populations and was not shown to be a statistically significant parameter.

Statistical analysis of the MBF parametric images using the generalized gamma probability density function also indicated increases in the parameters examined. Results for the generalized gamma *a* parameters (which can be linked to the effective scatterer cross-section; ref. 30) implied increases of 3.0 ± 0.5 A.U. (arbitrary unit), 6.0 ± 1.3 A.U., 14.8 ± 3.0 A.U., 4.0 ± 1.2 A.U. in positively responding patients in the first, fourth, eighth week of treatment, and preoperatively, respectively. Nonresponding patients had measured increases of 2.3 ± 0.8 A.U., 4.1 ± 1.7 A.U., 3.5 ± 1.9 A.U., 3.3 ± 0.9 A.U. in the first, fourth, eighth week of treatment, and preoperatively, respectively. Statistical analysis conducted on the changes observed in the generalized gamma *a* parameter indicated a statistically significant difference in the eighth week of treatment ($P = 0.046$). The changes in the generalized gamma c/v parameter (which can

Published OnlineFirst February 20, 2013; DOI: 10.1158/1078-0432.CCR-12-2965

Table 2. Ultimate responses of patients according to the clinical and pathologic reports

Patient	Residual tumordimensions (AP x ML x SI) in cm	Notes	Clinical/Pathologic Response
1	N/A	Complete pathologic response	Good
2	7 × 5 × 3	Carcinoma with mucinous features: very low cellularity	Good
3	2.7 × 2.5 × 2.4	Tumor cellularity remains very high	Poor
4	1.6 × 0.8 × 0.5	Good response	Good
5	N/A	Complete pathologic response	Good
6	3 × 6.4 × 3.5	High-grade invasive ductal carcinoma	Poor
7	N/A	Complete pathologic response	Good
8	1.4 × 1 × 1	Small volume of invasive tumor remaining	Good
9	11.4	Extensive residual disease	Poor
10	N/A	Complete pathologic response with only fibrous tumor bed remaining	Good
11	6.5 × 3 × 7.3	Invasive ductal carcinoma remaining	Poor
12	All the breast	Residual tumor took up all the breast: no response	Poor
13	4	Good response	Good
14	2 × 1.5 × 1	Complete pathologic response with only *in situ* disease remaining	Good
15	0.2 × 0.2	Complete pathologic response, with only in situ disease remaining	Good
16	3.5 × 2.3 × 1.3	Only *in situ* carcinoma with one focus of microinvasion (≤0.1 cm)	Good
17	6.5	Exceedingly low cellularity, thus overall tumor volume is also very low	Good
18	2.9 × 2 × 1.5 & 2 × 1.5 × 1	Tumor cellularity is low	Good
19	8 × 7.5 × 6	Good reduction in the tumor size	Good
20	N/A	Complete pathologic response	Good
21	6.5 × 5.5	Good reduction in the tumor size	Good
22	12.5 × 4.5 × 3.5	No definite response	Poor
23	N/A	No residual invasive carcinoma in the breast, only lymphovascularinvasion remaining	Good
24	N/A	Complete pathologic response, only scattered *in situ* component remaining	Good

be linked to the effective scatterer number density; ref. 30) were not found to be statistically significantly different between the 2 treatment groups.

Linear discriminant analyses (Fig. 4) were conducted to evaluate the separability of the 2 patient populations based on their clinical/pathologic response to the treatment, using the changes in the quantitative ultrasound parameters measured in fourth and eighth week of treatment. Results are summarized in Table 3. For the linear combination of MBF and 0-MHz intercept, the analyses resulted in sensitivities (percentage of nonresponders identified correctly) and specificities (percentage of responders identified correctly) of 100.0% and 83.3% at week 4, and 100% and 66.7% at week 8, respectively. Figure 4 shows the scatter plots of the patient data in the MBF and 0-MHz intercept feature plane where the determined borders of the treatment response classes has been shown by dashed lines. The plots show separations on responders versus nonresponding patients at weeks 4 and 8 that were statistically significant ($P = 0.02$), and approaching statistical significance ($P = 0.08$), respectively.

Discussion

The results presented in this study show for the first time that conventional frequency ultrasound may be clinically used to evaluate patient responses to cancer therapy regimens noninvasively. This study monitored 24 women through the course of their neoadjuvant chemotherapy treatment. Changes in the quantitative ultrasound spectral parameters were measured for each patient over the course of treatment. In contrast to the clinical/pathologic nonresponding patient population, considerable increases were observed in a number of quantitative ultrasound parameters obtained from the patient population which responded to the treatment, according to the clinical/pathologic reports. The fact that patients who responded poorly to treatment exhibited slight increases in tumor echogenicity (implied by

Published OnlineFirst February 20, 2013; DOI: 10.1158/1078-0432.CCR-12-2965

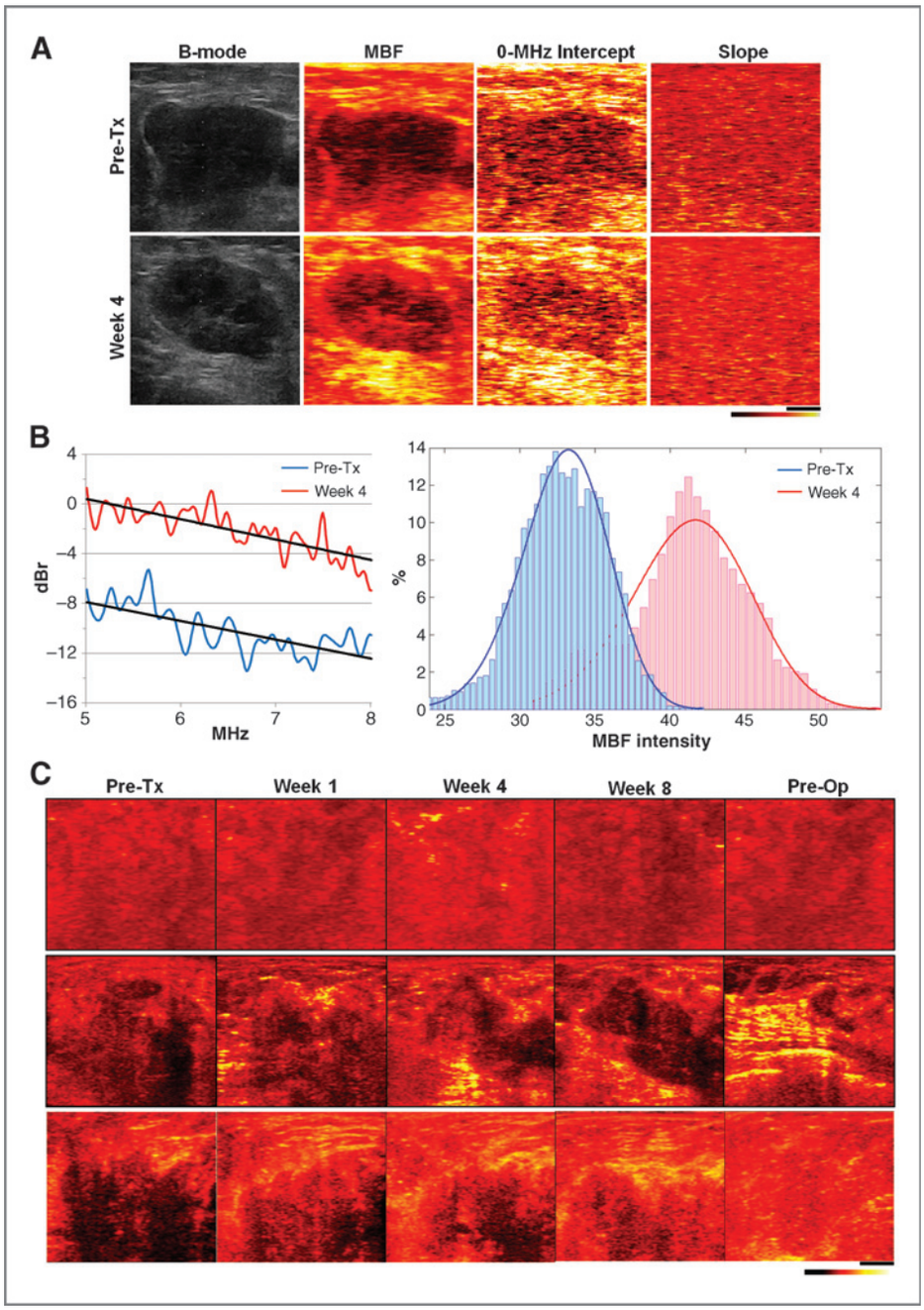

Figure 1. A, representative data from a large breast tumor before starting the neoadjuvant chemotherapy (first row), and after 4 weeks of treatment (second row). The columns from left to right show ultrasound B-mode, and parametric images of MBF, 0-MHz intercept, and spectral slope, respectively. The scale bar is approximately 1 cm, and the color map represents a scale encompassing approximately 50 dBr for MBF and 0-MHz intercept, and approximately 15 dBr/MHz for the spectral slope. B, normalized power spectra (left) and generalized gamma fits on the histograms of the MBF intensity (right) for the tumor region. C, representative parametric images of 0-MHz intercept from a nonresponding patient (first row), as well as from 2 patients that responded to the treatment (second and third rows). The data for each patient were acquired from the same nominal tumor regions before treatment as well as at weeks 1, 4, and 8 during treatment, and preoperatively from left to right, respectively. The scale bar represents approximately 1 cm. The color bar represents a scale encompassing approximately 80 dBr.

small increases in MBF and 0-MHz intercept parameters) is not surprising, as it is likely due to the fact that there was some limited response to chemotherapy which was detected. Statistically significant differences were exhibited between the 2 treatment response populations by the determined spectral and statistical parameters, after 4 and 8 weeks of treatment, respectively, but not as early as one week. This reflects observations in the clinic in which patients with an ultimately positive response to treatment may exhibit changes in tumor morphology on the macroscopic level within the first few weeks of treatment.

Linear discriminate analysis conducted suggested a favourable separability of the two treatment response populations using quantitative ultrasound spectral parameters acquired at weeks 4 and 8 of chemotherapy. The combination of MBF and 0-MHz intercept parameters distinguished between clinical responders and nonresponding patients with 100% sensitivity and 83.3% specificity at week 4, and 100% sensitivity and 66.7% specificity at week 8. These promising results imply that quantitative ultrasound spectral parameters can be applied for the early prediction of ultimate treatment response in patients undergoing cancer-

Published OnlineFirst February 20, 2013; DOI: 10.1158/1078-0432.CCR-12-2965

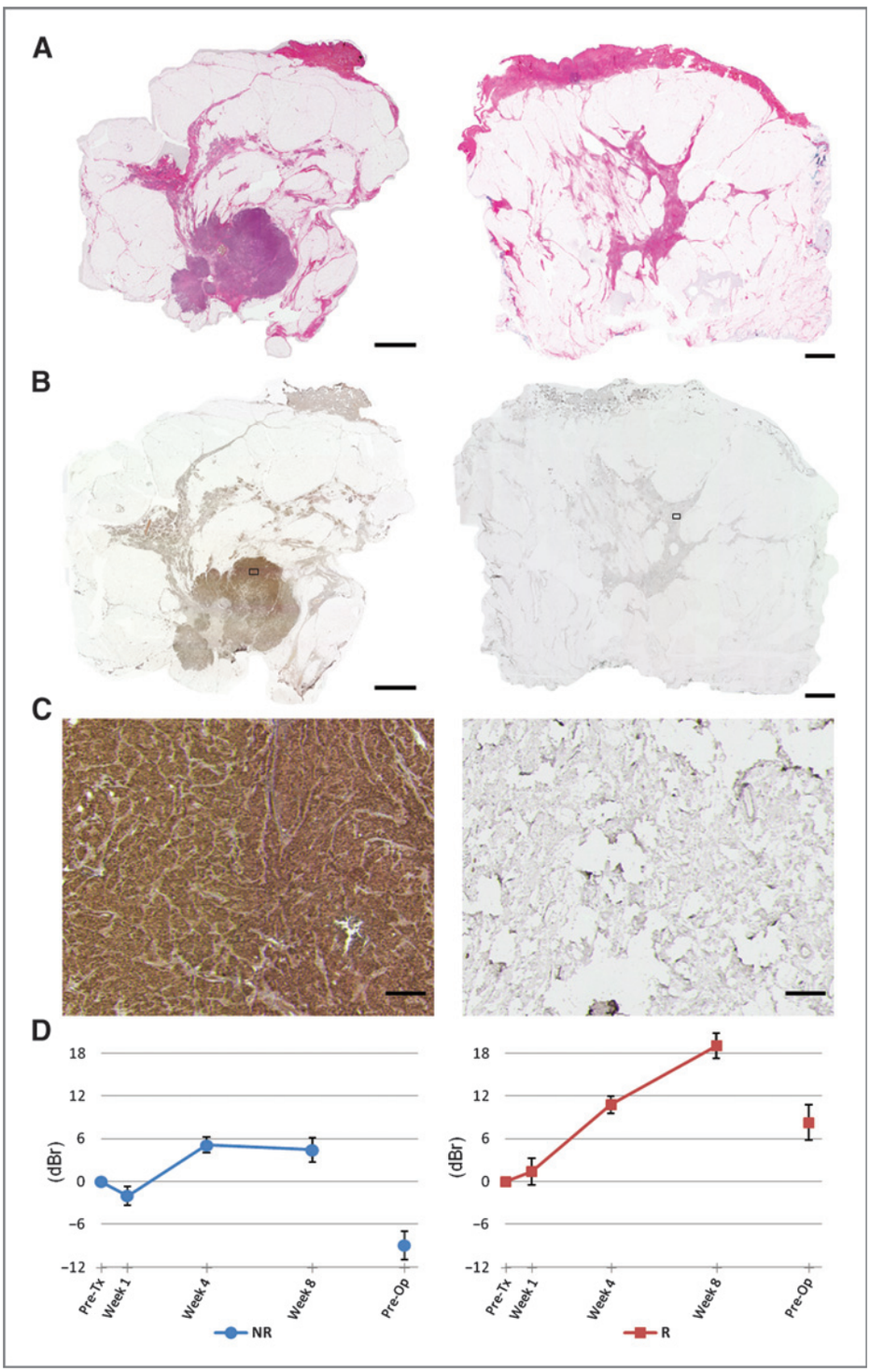

Figure 2. Representative data obtained from a nonresponder (left) and a responding patient (right). Both patients were initially confirmed with an ER+ status according to the pathology reports on core biopsy samples. A–C, light microscopy images of whole-mount histopathology slides obtained following modified radical mastectomy surgery. The scale bars are approximately 1 cm in A and B, and approximately 200 μm in C. A, H&E-stained slides. B, the immunohistochemical-stained slides highlighting ER+ areas. C, high magnification images of the areas marked with rectangles in B. Contrary to the case of the responding patient, the whole-mount pathology sample corresponding to the nonresponder patient indicates a large compact residual mass in the mastectomy specimen. D, results for the MBF measured in the same patients over the course of treatment. Data were measured before treatment onset, at weeks 1, 4, and 8 during treatment, and preoperatively.

targeting therapies. Such an early prediction could be used to facilitate the critical decision of switching to a more effective therapy for the treatment refractory patients early during the course of treatment.

Changes in the quantitative ultrasound spectral parameters from the baseline are expected to mainly show the development of response (apoptotic cell death) for each patient (as further discussed below). At the eighth week of treatment, the nonresponding patients may exhibit a late slight response to the treatment. In addition, a number of partial responders may have their tumor cells repopulated in partial regions showing small response levels. As such,

Published OnlineFirst February 20, 2013; DOI: 10.1158/1078-0432.CCR-12-2965

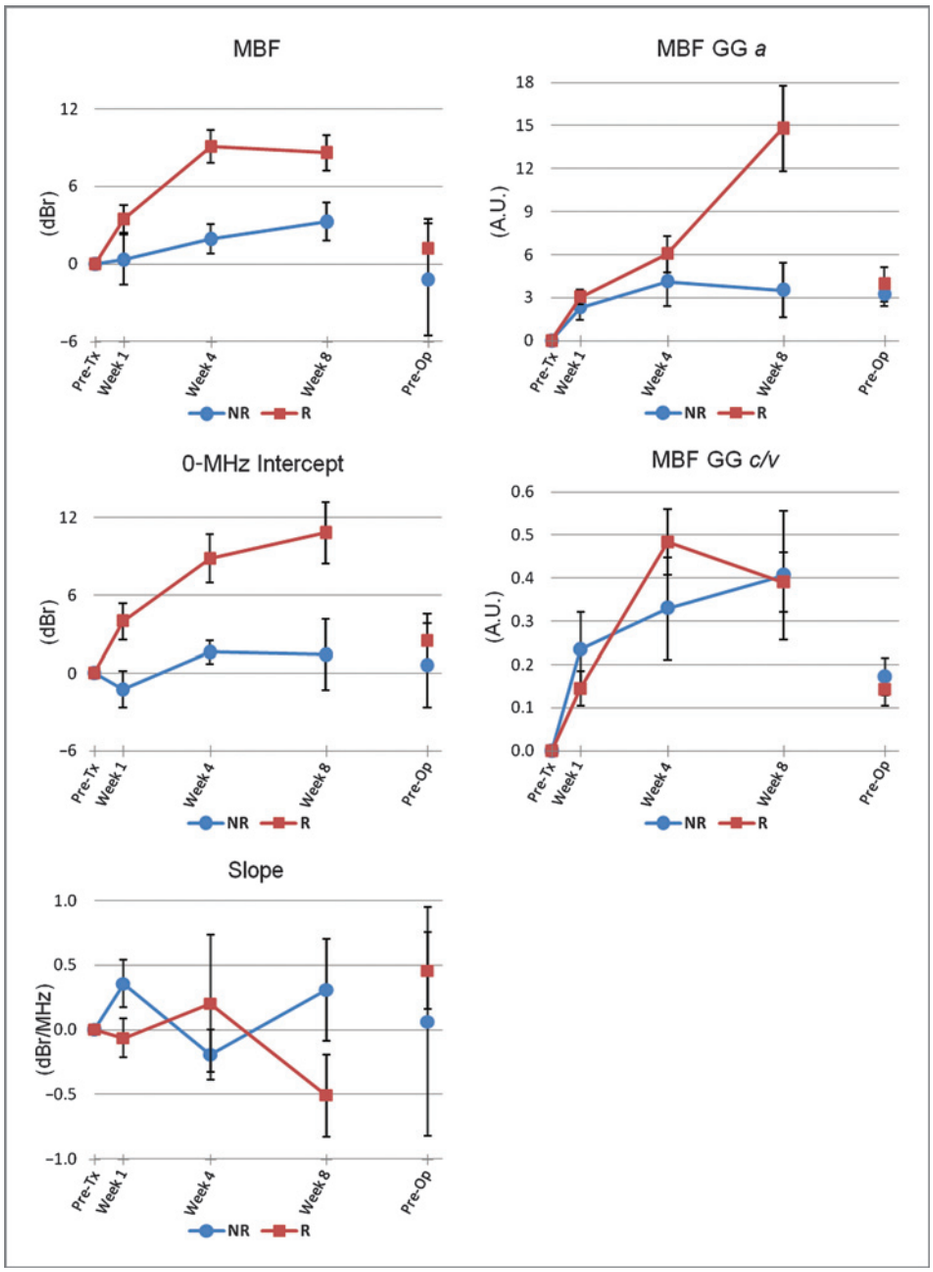

Figure 3. Average data obtained from treatment responding and nonresponding patients during treatment, for the MBF, 0-MHz intercept, and spectral slope, in addition to *a* and *c/v* parameters of the generalized gamma distribution fitted to the histogram of the MBF intensity. Data were measured before treatment onset, at weeks 1, 4, and 8 during treatment, and preoperatively. Blue lines display results obtained from patients who were clinically/pathologically categorized as nonresponders, whereas red lines display results obtained from responding patients. Error bars represent ± one SE.

having a relatively less separability between responding and nonresponding patient populations can be expected. Results obtained in this study (Fig. 3) showed a lesser separability between these 2 patient populations before surgery (pre-op). This may be happening due to the fact that at this time, the neoadjuvant chemotherapy has been stopped for several weeks, and thus minimal cell death is expected. Also, the complete pathologic responders who have no residual tumor left in ultrasound scans are not expected to show response and are excluded from the analysis at that time.

Previous *in vitro* and *in vivo* investigations of ultrasound-based cell death detection support the results presented in this study. The previous studies include those investigations where apoptosis was induced in cells and normal tissues using a variety of modalities and were analyzed using ultrasound data (7–14). It was shown that nuclear condensation by the induction of apoptotic death can result in increases in ultrasonic backscatter signal intensity, which is consistent with observations in this study. One might anticipate that measurable changes in backscatter characteristics from micron-sized particles are not expected at low frequencies, essentially because of the weak scattering strength of small-size scatterers. However, bulk changes in tissue associated with tumor cell death are principally

Published OnlineFirst February 20, 2013; DOI: 10.1158/1078-0432.CCR-12-2965

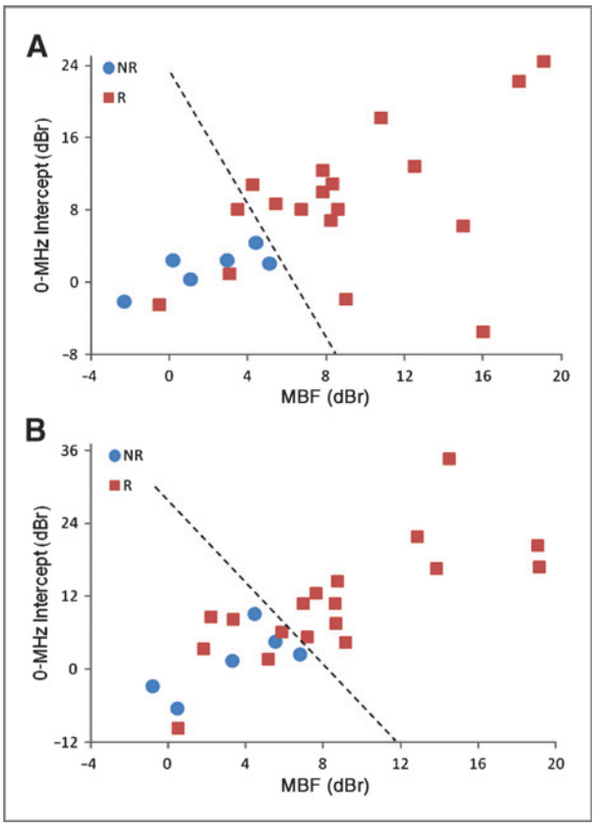

Figure 4. Scatter plot of the MBF and 0-MHz intercept data acquired at week 4 (A) and week 8 (B) of the chemotherapy treatment (changes compared to pretreatment). Responsive and nonresponding patients have been classified in the feature plane via a linear discriminant analysis where the determined border of classes has been shown by a dashed line.

related to alterations in the ensembles of cells and nuclei smaller than the wavelength of the ultrasound in the low- to mid-frequency range (near 10 MHz). Cell death introduces significant alterations in nuclear structures within these ensembles in addition to cellular changes in elasticity and viscosity as well as density (13). Acoustic properties of such ensembles are influenced by all of these alterations affecting ultrasound backscatter characteristics consequently. The potential scatterers are about 10 times smaller than the interrogating wavelength (10–30 μm vs. 100–200 μm), with sizes closer to those that predominate in the Rayleigh scattering regime (related to f^4, where f is frequency; ref. 31). Speckle patterns still forming at these low frequencies also suggest that several subresolution scatterers contribute to the detected signals. Another factor which can also influence ultrasound backscatter characteristics is the spatial organization of cellular-based scatterers (32) which can be altered with cell death. Banihashmei and colleagues showed that these subresolution scatterers can affect ultrasound at low-frequency with cell death (13) and evidence for the role of cell death–related nuclear changes is summarized there.

In this study, changes in the MBF and the 0-MHz intercept followed general trends experimentally observed for higher ultrasound frequencies. Effects of larger scattering structures can affect the spectral slope and its invariance suggests than both small and large scattering structures play a role at these frequencies. We have previously shown slope changes but only at high ultrasound frequencies (>20 MHz), when small scattering structures change their size (13). Attenuation was accounted for in this study by a sliding window normalization process against a tissue-mimicking phantom under similar scan settings for every scan. In addition, the 0-MHz intercept sensitive to the concentration of acoustic scatterers was determined parametrically for scans as it is theoretically believed to be free of attenuation effects (16).

Applications of other noninvasive imaging modalities for cancer treatment response monitoring have been investigated in previous studies, including those based on positron emission tomography (PET), MRI, or diffuse optical imaging and spectroscopy (6, 33–35). Unlike PET- and MRI-based methods, the ultrasound method here relies on inherent contrast changes arising from changes in acoustical properties as cancer cells die; hence, it does not need the injection of any external contrast agents. Diffuse optical spectroscopy has recently been used to show the capability of distinguishing between treatment responsive and nonresponding patients at the fourth week of chemotherapy (34). However, its lower resolution may lead to uncertainties for determining the tumor boundaries specially in the case of smaller tumors. Ultrasound has the advantages of low cost, rapid imaging speed, high resolution, and portability and can access tumor location not easily visualized with that modality.

Table 3. Results of the discriminant analyses conducted at weeks 4 and 8.

	Week 4		Week 8	
	Sensitivity	**Specificity**	**Sensitivity**	**Specificity**
MBF	100%	72.2%	83.3%	66.7%
0-MHz Intercept	100%	77.8%	83.3%	66.7%
Slope	66.7%	38.9%	50%	61.1%
Parametric MBF GG *a*	66.7%	38.9%	100%	66.7%
Parametric MBF GG *c/v*	66.7%	66.7%	66.7%	66.7%
MBF and 0-MHz intercept	100%	83.3%	100%	66.7%

Published OnlineFirst February 20, 2013; DOI: 10.1158/1078-0432.CCR-12-2965

In conclusion, this study indicates for the first time that conventional frequency quantitative ultrasound spectroscopic techniques can be clinically used to monitor treatment response in patients receiving cancer-targeting chemotherapy. Obtained results indicate that contrary to the case of treatment-refractory patients where quantitative ultrasound parameters were relatively invariant, the quantitative ultrasound parameters showed a considerable change for the patients who responded to treatment. Statistically significant differences were found after 4 to 8 weeks of chemotherapy onset. The quantitative ultrasound parameters used as response metrics were also found to have a favorable sensitivity and specificity to identify patients with poor ultimate response to therapy, early following treatment onset. As such, this work is a substantial forward step toward clinical application of quantitative ultrasound as early surrogate of ultimate treatment response for patients with cancer. Such a surrogate may facilitate personalized cancer therapy where an inefficient treatment regimen for a particular patient is switched to a more effective one, early after the therapy initiation, or early salvage treatment is undertaken. Nevertheless, investigations on larger cohorts of patients will be required to assess the efficacy of the proposed technique for distinguishing between subtypes of treatment response, and to further evaluate the robustness of the technique in clinic.

Disclosure of Potential Conflicts of Interest

No potential conflicts of interest were disclosed.

Authors' Contributions

Conception and design: A. Sadeghi-Naini, N. Papanicolau, J. Zubovits, R. Dent, S. Verma, J.F. Boileau, J. Spayne, E. Sofroni, M.C. Kolios, G.J. Czarnota
Development of methodology: A. Sadeghi-Naini, N. Papanicolau, J. Zubovits, E. Sofroni, M.C. Kolios, G.J. Czarnota
Acquisition of data (provided animals, acquired and managed patients, provided facilities, etc.): A. Sadeghi-Naini, N. Papanicolau, O. Falou, J. Zubovits, M.E. Trudeau, S. Iradji, E. Sofroni, J. Lee, G.J. Czarnota
Analysis and interpretation of data (e.g., statistical analysis, biostatistics, computational analysis): A. Sadeghi-Naini, N. Papanicolau, O. Falou, M.J. Yaffe, G.J. Czarnota
Writing, review, and/or revision of the manuscript: A. Sadeghi-Naini, N. Papanicolau, M.E. Trudeau, M.J. Yaffe, G.J. Czarnota
Administrative, technical, or material support (i.e., reporting or organizing data, constructing databases): A. Sadeghi-Naini, R. Dent, S. Verma, J.F. Boileau, J. Spayne, S. Lemon-Wong, M.C. Kolios
Study supervision: A. Sadeghi-Naini, G.J. Czarnota

Grant Support

This study was funded, in part, by the Canadian Breast Cancer Foundation—Ontario Region through fellowships awarded to A. Sadeghi-Naini and O. Falou, and through a research grant to G.J. Czarnota. Funding for this project was also provided by the Terry Fox Foundation and the Natural Sciences and Engineering Research Council of Canada. This work was also supported though a Cancer Care Ontario Research Chair in experimental therapeutics and imaging awarded to G.J. Czarnota.

The costs of publication of this article were defrayed in part by the payment of page charges. This article must therefore be hereby marked *advertisement* in accordance with 18 U.S.C. Section 1734 solely to indicate this fact.

Received September 14, 2012; revised January 18, 2013; accepted February 3, 2013; published OnlineFirst February 20, 2013.

References

1. American Cancer Society. Cancer facts and figures 2012. Atlanta, GA: American Cancer Society; 2012.
2. Korourian S, Klimberg S, Henry-Tillman R, Lindquist D, Jones M, Eng DC, et al. Assessment of proliferating cell nuclear antigen activity using digital image analysis in breast carcinoma following magnetic resonance-guided interstitial laser photocoagulation. Breast J 2003;9:409–13.
3. Mankoff DA, Dunnwald LK, Gralow JR, Ellis GK, Drucker MJ, Livingston RB. Monitoring the response of patients with locally advanced breast carcinoma to neoadjuvant chemotherapy using [technetium 99m]-sestamibi scintimammography. Cancer 1999;85:2410–23.
4. Giordano SH. Update on locally advanced breast cancer. Oncologist 2003;8:521–30.
5. Segel MC, Paulus DD, Hortobagyi GN. Advanced primary breast cancer: assessment at mammography of response to induction chemotherapy. Radiology 1988;169:49–54.
6. Brindle K. New approaches for imaging tumour responses to treatment. Nat Rev Cancer 2008;8:94–107.
7. Czarnota GJ, Kolios MC, Vaziri H, Benchimol S, Ottensmeyer FP, Sherar MD, et al. Ultrasonic biomicroscopy of viable, dead and apoptotic cells. Ultrasound Med Biol 1997;23:961–5.
8. Czarnota GJ, Kolios MC, Abraham J, Portnoy M, Ottensmeyer FP, Hunt JW, et al. Ultrasound imaging of apoptosis: high-resolution non-invasive monitoring of programmed cell death *in vitro*, *in situ* and *in vivo*. Br J Cancer 1999;81:520–7.
9. Kolios MC, Czarnota GJ, Hussain M, Foster FS, Hunt JW, Sherar MD. Analysis of ultrasound backscatter from ensembles of cells and isolated nuclei. In: Proceedings of IEEE Ultrasonics Symposium; 2001 Oct 7–10; Atlanta, GA. New York, NY: IEEE; 2001. p. 1257–60.
10. Tunis AS, Czarnota GJ, Giles A, Sherar MD, Hunt JW, Kolios MC. Monitoring structural changes in cells with high-frequency ultrasound signal statistics. Ultrasound Med Biol 2005;31:1041–9.
11. Taggart LR, Baddour RE, Giles A, Czarnota GJ, Kolios MC. Ultrasonic characterization of whole cells and isolated nuclei. Ultrasound Med Biol 2007;33:389–401.
12. Vlad RM, Alajez NM, Giles A, Kolios MC, Czarnota GJ. Quantitative ultrasound characterization of cancer radiotherapy effects *in vitro*. Int J Radiat Oncol Biol Phys 2008;72:1236–43.
13. Banihashemi B, Vlad R, Debeljevic B, Giles A, Kolios MC, Czarnota GJ. Ultrasound imaging of apoptosis in tumor response: novel preclinical monitoring of photodynamic therapy effects. Cancer Res 2008;68:8590–6.
14. Vlad RM, Brand S, Giles A, Kolios MC, Czarnota GJ. Quantitative ultrasound characterization of responses to radiotherapy in cancer mouse models. Clin Cancer Res 2009;15:2067–75.
15. Lizzi FL, Ostromogilsky M, Feleppa EJ, Rorke MC, Yaremko MM. Relationship of ultrasonic spectral parameters to features of tissue microstructure. IEEE Trans Ultrason Ferroelectr Freq Control 1987;34:319–29.
16. Lizzi FL, Astor M, Liu T, Deng C, Coleman DJ, Silverman RH. Ultrasonic spectrum analysis for tissue assays and therapy evaluation. Int J Imaging Syst Technol 1997;8:3–10.
17. Oelze ML, O'Brien WD, Blue JP, Zachary JF. Differentiation and characterization of rat mammary fibroadenomas and 4T1 mouse carcinomas using quantitative ultrasound imaging. IEEE Trans Med Imaging 2004;23:764–71.
18. Feleppa EJ, Kalisz A, Sokil-Melgar JB, Lizzi FL, Rosado AL, Shao MC, et al. Typing of prostate tissue by ultrasonic spectrum analysis. IEEE Trans Ultrason Ferroelectr Freq Control 1996;43:609–19.
19. Yang M, Krueger TM, Miller JG, Holland MR. Characterization of anisotropic myocardial backscatter using spectral slope, intercept and midband fit parameters. Ultrason Imaging 2007;29:122–34.
20. Guimond A, Teletin M, Garo E, D'Sa A, Selloum M, Champy M-F, et al. Quantitative ultrasonic tissue characterization as a new tool for

Published OnlineFirst February 20, 2013; DOI: 10.1158/1078-0432.CCR-12-2965

continuous monitoring of chronic liver remodelling in mice. Liver Int 2007;27:854–64.
21. Azrif M, Ranieri S, Giles A, Debeljevic B, Kolios MC, Czarnota GJ. Conventional low-frequency ultrasound detection of apoptosis [abstract]. In: Proceedings of the American Institute of Ultrasound in Medicine Annual Convention; 2007. New York, NY. p. S185.
22. Sadeghi-Naini A, Falou O, Czarnota GJ. Detecting cancer treatment response using textural properties of quantitative ultrasound parametric maps: migrating from high-frequencies to the conventional-frequencies [abstract]. In: Proceedings of the 8th International Conference on Ultrasonic Biomedical Microscanning (UBM); 2012 St-Paulin, Quebec, Canada.
23. Falou O, Sadeghi-Naini A, Czarnota GJ. Using high- and conventional-frequency ultrasound for the detection of cell death in mouse models after chemotherapy [abstract]. In: Proceedings of the 8th International Conference on Ultrasonic Biomedical Microscanning (UBM); 2012. St-Paulin, Quebec, Canada.
24. Clarke GM, Eidt S, Sun L, Mawdsley G, Zubovits JT, Yaffe MJ. Whole-specimen histopathology: a method to produce whole-mount breast serial sections for 3-D digital histopathology imaging. Histopathology 2007;50:232–42.
25. Therasse P, Arbuck SG, Eisenhauer EA, Wanders J, Kaplan RS, Rubinstein L, et al. New guidelines to evaluate the response to treatment in solid tumors. European Organization for Research and Treatment of Cancer, National Cancer Institute of the United States, National Cancer Institute of Canada. J Natl Cancer Inst 2000;92:205–16.
26. Dong F, Madsen EL, MacDonald MC, Zagzebski JA. Nonlinearity parameter for tissue-mimicking materials. Ultrasound Med Biol 1999;25:831–8.
27. Lizzi FL, Greenebaum M, Feleppa EJ, Elbaum M, Coleman DJ. Theoretical framework for spectrum analysis in ultrasonic tissue characterization. J Acoust Soc Am 1983;73:1366–73.
28. Feleppa EJ, Lizzi FL, Coleman DJ, Yaremko MM. Diagnostic spectrum analysis in ophthalmology: a physical perspective. Ultrasound Med Biol 1986;12:623–31.
29. Oelze ML, O'Brien WD. Method of improved scatterer size estimation and application to parametric imaging using ultrasound. J Acoust Soc Am 2002;112:3053–63.
30. Tunis AS. Monitoring structural changes in cells and tissues with high frequency ultrasound signal statistics. MSc Thesis; University of Toronto; 2005. p. 1–79.
31. Strutt JW. Investigation of the disturbance produced by a spherical obstacle on the waves of sound. Proc Lond Math Soc 1871;s1–4:253–83.
32. Hunt JW, Worthington AE, Xuan A, Kolios MC, Czarnota GJ, Sherar MD. A model based upon pseudo regular spacing of cells combined with the randomisation of the nuclei can explain the significant changes in high-frequency ultrasound signals during apoptosis. Ultrasound Med Biol 2002;28:217–26.
33. Sadeghi-Naini A, Falou O, Hudson JM, Bailey C, Burns PN, Yaffe MJ, et al. Imaging innovations for cancer therapy response monitoring. Imaging Med 2012;4:311–27.
34. Soliman H, Gunasekara A, Rycroft M, Zubovits J, Dent R, Spayne J, et al. Functional imaging using diffuse optical spectroscopy of neoadjuvant chemotherapy response in women with locally advanced breast cancer. Clin Cancer Res 2010;16:2605–14.
35. Falou O, Soliman H, Sadeghi-Naini A, Iradji S, Lemon-wong S, Zubovits J, et al. Diffuse optical spectroscopy evaluation of treatment response in women with locally advanced breast cancer receiving neoadjuvant chemotherapy. Transl Oncol 2012;5:238–46.